Proceedings of the
Annual Stability Conference
Structural Stability Research Council
Atlanta, Georgia, April 21-24, 2026

Design for stability of structural steel connections using the component-based finite element method

Mark D. Denavit[1], Javad Esmaeelpour[2], Martin Vild[3]

Abstract

Design for stability of structural steel connections requires consideration of the same physical effects critical for design of members and frames, including second-order effects, geometric imperfections, and stiffness reductions due to inelasticity. However, connections often have more complicated configurations and boundary conditions than members and frames. Connection design by advanced inelastic analysis using the component-based finite element method (CBFEM) has emerged as a powerful tool, especially for complex connections. Geometric imperfections and residual stresses are rarely modeled directly in CBFEM. Furthermore, CBFEM analyses are often geometrically linear. Therefore, additional steps are needed to design for stability using CBFEM. One approach is to pair the material nonlinear analysis with a linear buckling analysis and ensure that the buckling load exceeds the applied loads by a critical ratio. Since this approach does not directly model geometric imperfections and residual stresses, the ratio must be carefully selected to ensure safe designs, especially for connections susceptible to inelastic buckling. This study compares design for stability using CBFEM to traditional approaches using equations from the AISC *Specification for Structural Steel Buildings*. Several connection configurations are analyzed to evaluate a range of stability limit states. The critical buckling ratio limit needed to ensure safe designs using CBFEM is identified for the various configurations. The results of this study enable confident and efficient use of CBFEM for connections susceptible to stability limit states.

1. Introduction

AISC *Specification* (2022) Section C1 lists five major effects that must be considered in design for stability of structural steel systems and components, including steel yielding, residual stresses, geometric nonlinearity, and initial geometric imperfections. The section also notes that any rational method of design for stability that considers all of the effects is permitted. Such methods of design include traditional methods employing the strength equations in the *Specification* and advanced methods employing nonlinear finite element analyses.

[1] Associate Professor, University of Tennessee, Knoxville, <mdenavit@utk.edu>
[2] Graduate Research Assistant, University of Tennessee, Knoxville, <jesmaeel@vols.utk.edu>
[3] Associate Professor, Brno University of Technology, <martin.vild@vutbr.cz>

The traditional method of strength design for compression elements in structural steel connections uses the provisions of AISC *Specification* (2022) Section J4. This section addresses yielding and buckling with the nominal strength taken as $P_n = F_y A_g$ when $L_c/r \leq 25$ and the nominal strength determined using the provisions of AISC *Specification* Chapter E when $L_c/r > 25$. Neglecting strength reductions due to buckling when $L_c/r \leq 25$ simplifies design of connections and is justified because connection elements exhibit increased capacity stemming from lower residual stresses and different shapes compared to the typical columns for which the provisions of Chapter E were derived (Dowswell 2016).

The AISC column curve, defined by AISC *Specification* (2022) Eqs. E3-2 and E3-3, accounts for residual stresses and initial geometric imperfections, both of which reduce the strength in comparison to a rudimentary column curve for flexural buckling established by considering steel yielding and elastic buckling only. The AISC column curve was developed based on geometrically and materially nonlinear analysis with imperfections (GMNIA) results for a range of column shapes and lengths. GMNIA is considered the truest to reality and can account for all the effects listed in AISC *Specification* Section C1.

The traditional method works well for relatively simple connections and connecting elements where the compression is uniform and the effective length and required strength can be confidently defined. However, less common connections or those with more complex geometries often require the use of unproven assumptions to assess stability using the traditional approach leading to uncertainty.

Design by advanced inelastic analysis is another approach to structural steel connection design. The finite element analyses that underlie the approach allow flexible representation of geometry, which mitigates the need for ad hoc assumptions for specific connection types. The component-based finite element method (CBFEM) is an approach to design by inelastic analysis well-suited for design office use (Wald et al. 2020; Denavit et al. 2024). In the CBFEM connecting elements, such as plates and rolled shapes, are modeled with nonlinear shell elements, and bolts and welds are modeled as a series of special elements and nonlinear springs. The CBFEM typically employs a materially nonlinear analysis excluding the effects of geometric nonlinearity and initial geometric imperfections. Sometimes geometric nonlinearities are modeled, however, the CBFEM does not typically consider residual stresses, which can accentuate stiffness reductions due to partial yielding, nor does it consider initial geometric imperfections. Because these physical effects are not considered in the analysis, an additional check for buckling that considers these effects needs to be performed.

In the CBFEM, buckling is typically checked using the ratio between the critical buckling load and the applied load. This ratio is termed the buckling ratio or buckling factor and is denoted as α_{cr}. The buckling ratio must be greater than or equal to a minimum, limiting buckling ratio denoted as $\alpha_{cr,lim}$. The limiting buckling ratio depends on the type of buckling (e.g., global buckling vs local buckling) and material properties. It also depends on the design method used (i.e., LRFD vs ASD). A general recommendation for local buckling is that the buckling ratio should not be less than $3.0/\phi$ for LRFD or 3.0Ω for ASD where $\phi = 0.90$ and $\Omega = 1.67$. Higher limits for bracket plate connections, 4.0 for LRFD and 6.0 for ASD, have been identified through comparisons to

experimental results (Dowswell and Vild 2023) and other recommendations for plate elements vary based on the boundary conditions (IDEA StatiCa 2023).

In this study, comparisons were made between traditional methods for stability design using equations from the AISC *Specification* (2022) and an advanced method using the CBFEM. The goal of these comparisons was to quantify acceptable values of the limiting buckling ratio and identify limitations on the use of the CBFEM for stability design of structural steel connections. A range of limit states including Euler buckling, plate buckling, shear buckling, and web local crippling were investigated.

2. Euler Buckling

This section compares strength results from traditional calculations and the CBFEM for the limit states of compressive yielding and flexural buckling. This section also introduces the basic comparison approach used for other limit states in this study. The idealized connection investigated in this section features a plate connected between two wide flange members with end plates (Figure 1). The simple loading and boundary conditions of this connection allow for direct comparisons to strength equations.

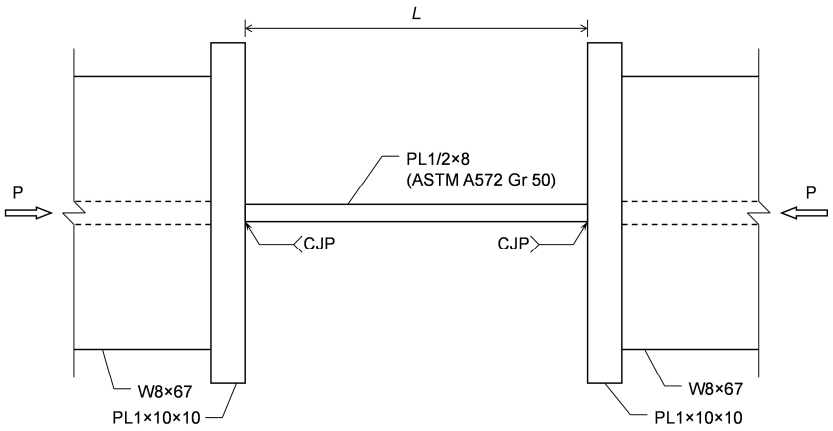

Figure 1: Idealized connection for investigation of Euler buckling

The plate is 1/2 in. thick, 8 in. wide, and connected to the end plates with complete joint penetration groove welds. The length of the plate varies. The boundary conditions are defined such that the rotations are fixed and translations are free resulting in a sidesway permitted (i.e., $K = 1$) buckled shape of the plate as shown in Figure 2.

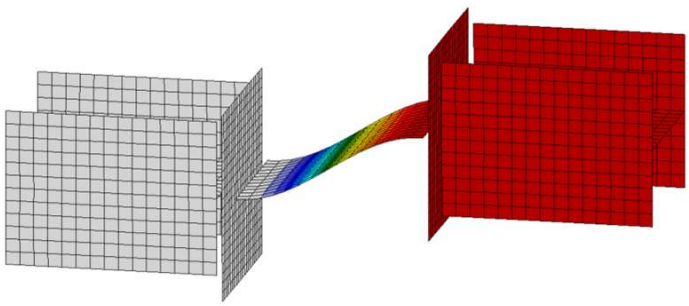

Figure 2: Buckled shape for Euler buckling in an idealized connection

CBFEM analyses were performed using IDEA StatiCa Connection (Version 25.0 using default settings, including for mesh parameters) for lengths, L, ranging from 2 in. to 16 in. Results from the analyses include the load at which the connection fails according to a first-order analysis, $P_{CBFEM,PL}$, and the critical elastic buckling load, $P_{CBFEM,e}$. The overall strength according to the CBFEM, P_{CBFEM} is the lesser of $P_{CBFEM,PL}$ and $P_{CBFEM,e}$ divided by $\alpha_{cr,lim}$.

$$P_{CBFEM} = \min\left(P_{CBFEM,PL}, P_{CBFEM,e}/\alpha_{cr,lim}\right) \tag{1}$$

Results from the CBFEM are compared to results from traditional calculations in Figure 3, where the elastic buckling strength is computed as

$$P_e = \frac{\pi^2 EI}{L^2} \tag{2}$$

where E is the modulus of elasticity, I is the moment of inertia, and L is the unbraced length for a pin-ended member. The design strength, ϕP_n, is computed using the provisions of AISC *Specification* (2022) Section J4 with $L_c = L$.

Pairs of comparable data can be seen in Figure 3: $\phi F_y A_g$ is comparable to $P_{CBFEM,PL}$ since both represent yielding strength; ϕP_n is comparable to P_{CBFEM} since both represent the design strength; and P_e is comparable to $P_{CBFEM,e}$ since both represent the elastic buckling strength. The yielding strengths are essentially the same except that $P_{CBFEM,PL}$ is greater than $\phi F_y A_g$ for $L_c \leq 4$ in. For very short plates, end restraint and the Poisson effect cause a more complicated multi-axial state of stress in the plate in the CBFEM model that results in greater strength. The elastic buckling strengths are essentially the same over the range investigated indicating that Eq. 2 matches the critical elastic buckling load of the CBFEM model.

The design strength varies between the two methods. When L_c = 2 in., $L_c/r \leq 25$ therefore compressive yielding controls the traditional strength calculations. Yielding also controls the CBFEM strength and, as noted previously, the CBFEM yielding strength for the plate is greater than the traditional strength. For L_c = 4 and 6 in. ($L_c/r > 25$) flexural buckling controls the traditional strength calculations, however, yielding still controls the CBFEM strength with $\alpha_{cr,lim} = 3.0/\phi$, as shown in Figure 3(a). For $L_c \geq 8$ in. and $\alpha_{cr,lim} = 3.0/\phi$, flexural buckling controls the traditional strength calculations and the buckling limit controls the CBFEM strength. In this range, $P_{CBFEM} = \phi P_e/3.0$ which is much less than ϕP_n.

For buckling to control the CBFEM strength at $L_c/r = 25$, the limiting buckling ratio would need to be:

$$\alpha_{cr,lim} = \frac{1}{\phi F_y}\frac{\pi^2 E}{25^2} \tag{3}$$

For F_y = 50 ksi, this limiting value is $\alpha_{cr,lim} = 9.2/\phi$. Results using this limiting value are shown in Figure 3(b). With $\alpha_{cr,lim} = 9.2/\phi$, the critical buckling ratio limit controls for all lengths where flexural buckling controls the traditional calculations. The CBFEM strength results in this range

of lengths are very conservative. Experimental testing would be beneficial to determine if such a high value of the critical buckling ratio limit is truly necessary. However, as a point of comparison, Section 5.2.1 of Eurocode 3 (CEN 2005) defines $\alpha_{cr,lim} = 15$ for design of frames by plastic analysis.

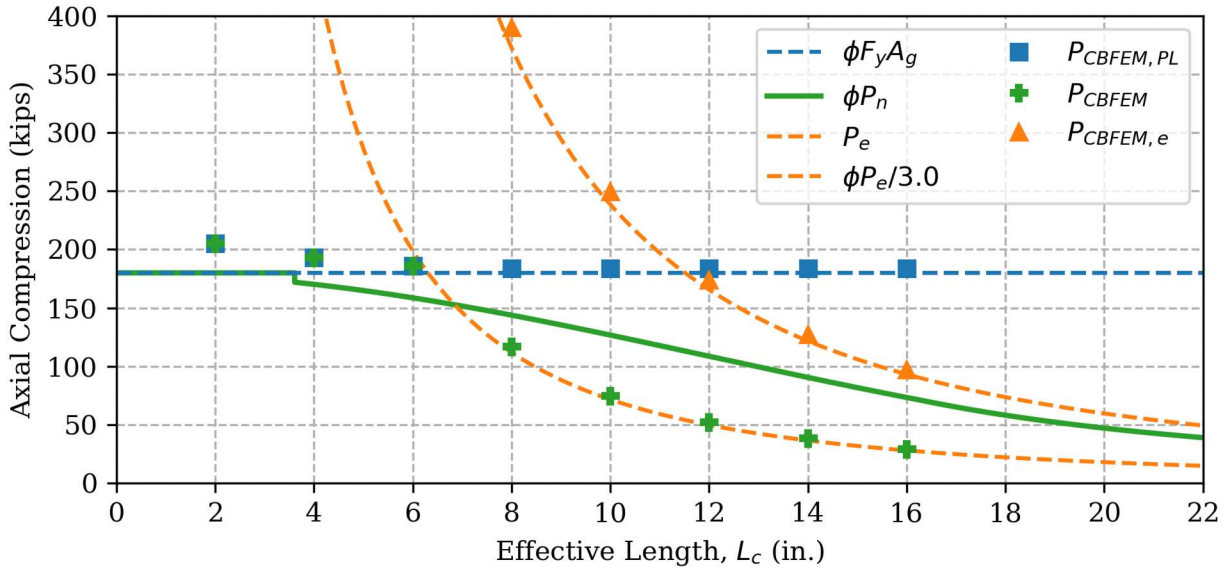

(a) with $\alpha_{cr,lim} = 3.0/\phi$

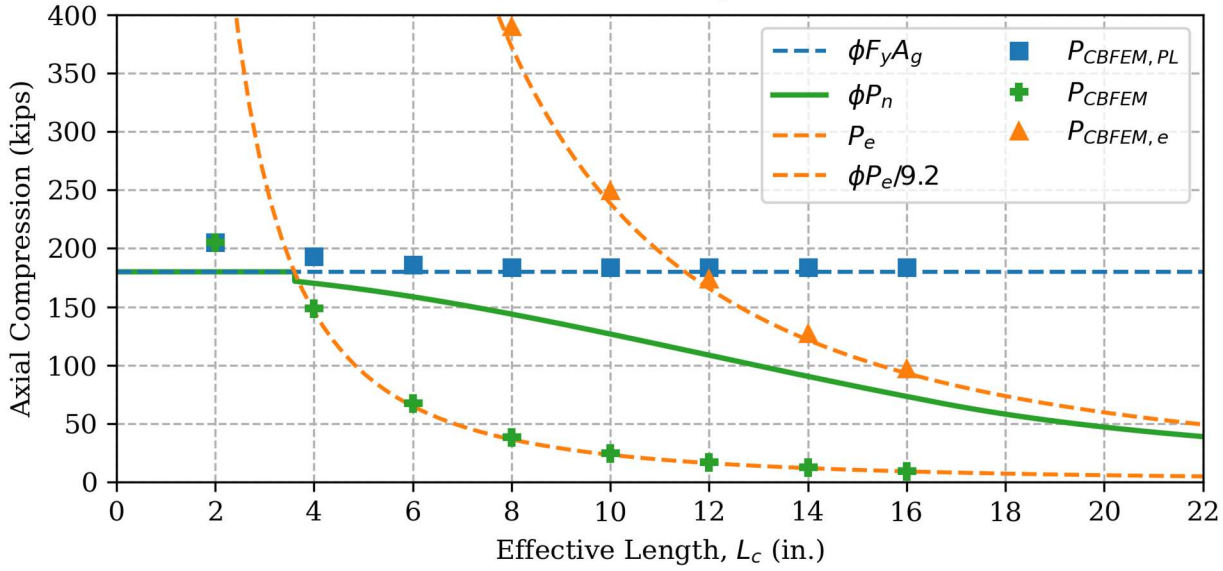

(b) with $\alpha_{cr,lim} = 9.2/\phi$

Figure 3: Strength comparison for Euler buckling

3. Plate Buckling

Plate elements in connections that have boundary conditions along more edges than investigated in the previous section can also experience flexural buckling. AISC *Specification* (2022) Chapter J does not contain detailed provisions for plate buckling, however, Chapters E and F have provisions for plate buckling in the context of local buckling. While these provisions are for members, they provide a useful point of comparison. Two conditions are evaluated in this section: square hollow structural sections (HSS) subject to axial compression and built-up I-shaped sections subject to flexure.

The square HSS investigated has F_y = 50 ksi and outside dimensions of 8 in. by 8 in. The thickness of the wall, t, was varied. In the CBFEM model, the HSS was modeled as an 18 in. long segment between two end plates welded to stiff members as shown in Figure 4. The HSS was CJP welded to the end plates.

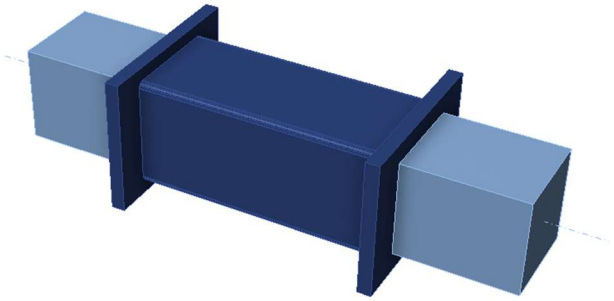

Figure 4: Connection for investigation of plate buckling in a HSS compression member

Results for this HSS stub are shown in Figure 5 with respect to the wall width-to-thickness ratio, b/t where b = 8 in. – 3t due to the rounded corners. The results are presented in a similar manner as in Figure 3. Strength results are normalized by cross-sectional area so that the yielding strength is constant. The design strength, ϕP_n, was computed using the provisions of AISC *Specification* (2022) Section E7 including calculation of the effective width of the walls of the HSS with the assumption that $F_n = F_y$ (i.e., no member length stability reduction). The elastic local buckling stress, F_{el}, was computed using AISC *Specification* Eq. E7-5.

With the normalization of the strength results, the design yielding strength is constant at ϕF_y. The CBFEM yielding strength is constant at a slightly higher value due to the small hardening stiffness assumed in the nonlinear analysis model. The CBFEM buckling stress matches well with the elastic local buckling stress from the AISC *Specification* (2022). With $\alpha_{cr,lim} = 3.0/\phi$, the CBFEM design strength is accurate or conservative in comparison to the AISC design strength across the whole range of width-to-thickness ratios. The conservativism is significant when the critical buckling limit controls the CBFEM strength. With $\alpha_{cr,lim} = 1.9/\phi$, a value selected such that the critical buckling limit controls only for sections classified as slender, the CBFEM results are less conservative. However, the limiting critical buckling ratio to achieve this result depends on F_y (the limiting ratio increases with increases in F_y).

For the second condition, the built-up I-shape investigated has F_y = 50 ksi, overall depth of d = 12 in., flange width of b_f = 6.52 in., and web thickness of t_w = 0.26 in. The thickness of the flanges, t_f, was varied. In the CBFEM model, the I-shape was modeled as two segments CJP welded to each other with a buckled shape as shown in Figure 6.

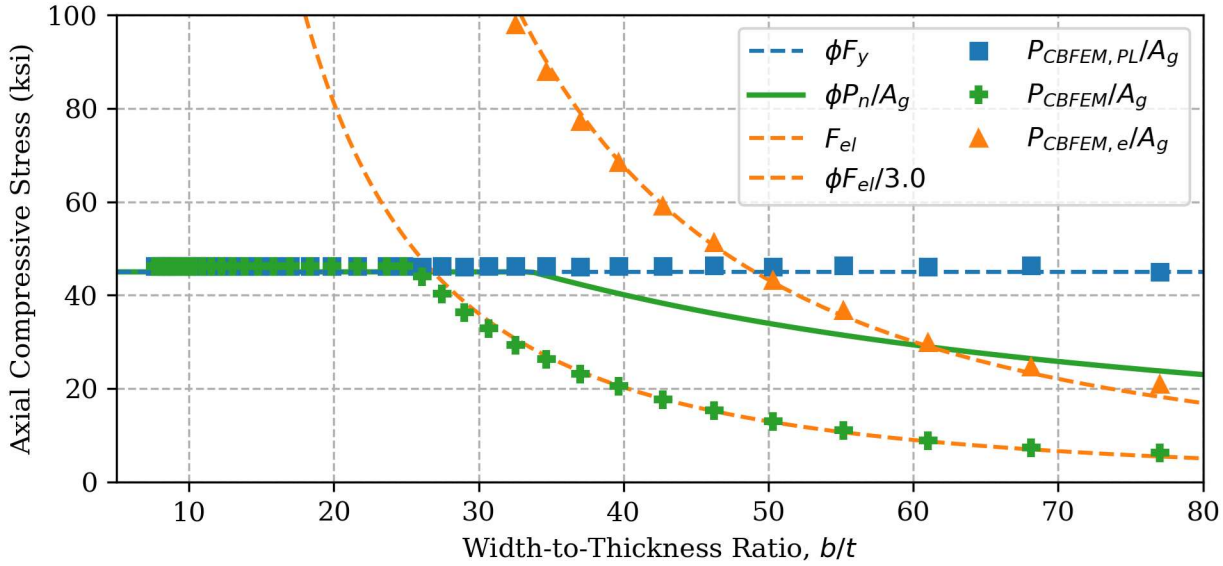

(a) with $\alpha_{cr,lim} = 3.0/\phi$

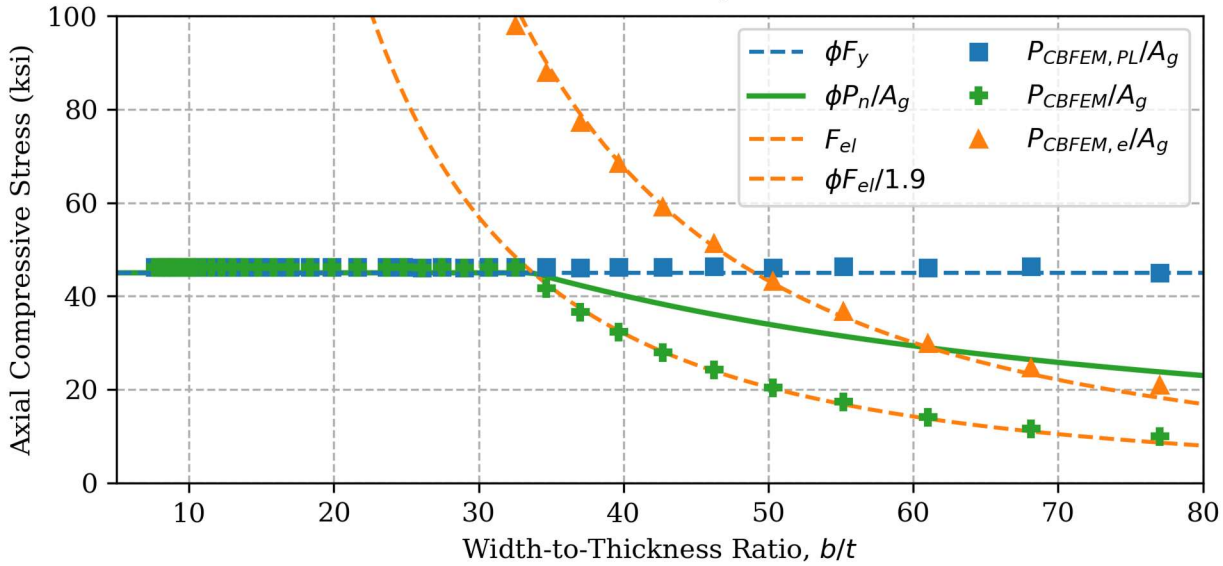

(b) with $\alpha_{cr,lim} = 1.9/\phi$

Figure 5: Strength comparison for plate buckling in a HSS compression member

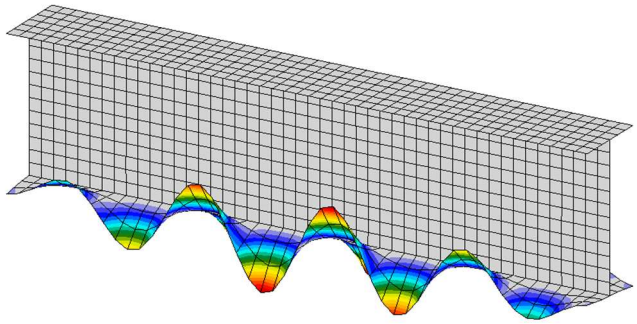

Figure 6: Buckled shape for plate buckling in a built-up I-shaped flexural member

Results for this connection are shown in Figure 7 with respect to the width-to-thickness ratio of the flange. The results are normalized by the plastic section modulus so that the yielding strength is constant. The design strength, ϕM_n, was computed using the provisions of AISC *Specification* (2022) Section F3. The elastic local buckling moment, M_{el}, was computed as the critical buckling stress according to Eq. 4 with k = 0.425, a value appropriate for one edge simply supported (ignoring the restraint provided by the web) and the other free (Young et al. 2011), and $b/t = b_f/2t_f$ times the elastic section modulus.

$$F_{el} = k\frac{\pi^2 E}{12\left(1-\nu^2\right)\left(b/t\right)^2} \tag{4}$$

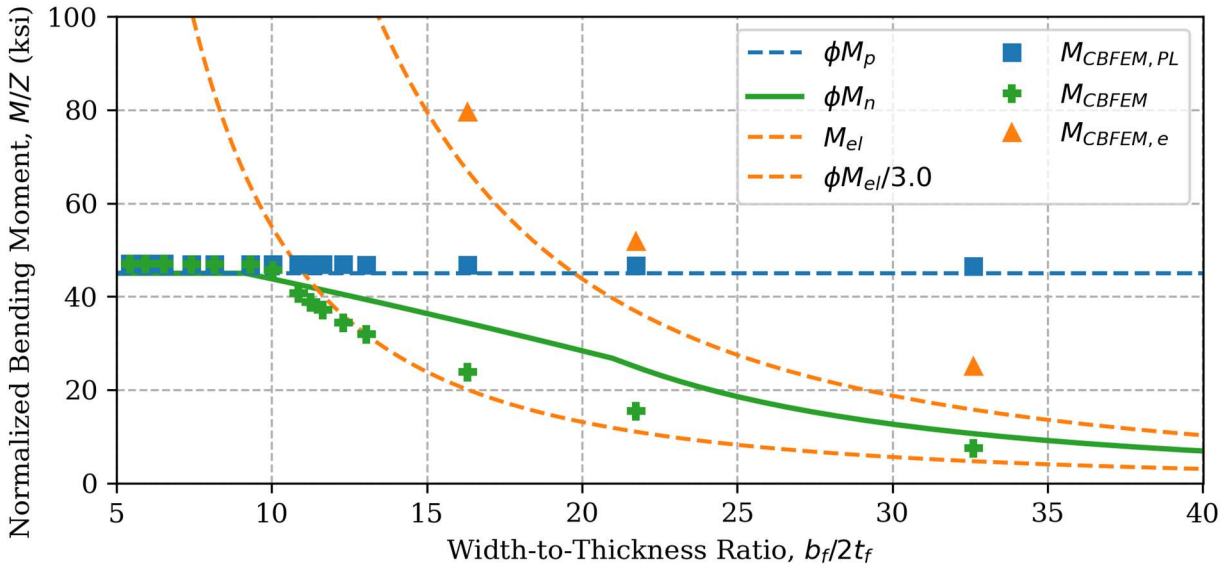

Figure 7: Strength comparison for plate buckling in a built-up I-shaped flexural member

As with the HSS compression member, the design yielding strength is constant at ϕF_y and the CBFEM yielding strength is constant at a slightly higher value. The CBFEM buckling stress is somewhat higher than the approximate value used in this study, primarily due to rotational restraint provided by the web not considered in the approximate value. With $\alpha_{cr,lim}$ = 3.0/ϕ, the CBFEM design strength is accurate or conservative in comparison to the AISC design strength across the whole range of width-to-thickness ratios. The critical buckling ratio limit controls for sections classified in the traditional method as noncompact or slender.

4. Shear Buckling

Shear buckling is another limit state that can apply to plate elements in connections. Again, given the lack of connection specific provisions for shear buckling, comparisons are made to member provisions in AISC *Specification* (2022) Chapter G. A built-up I-shaped member subject to major axis shear where yielding and buckling of the web are the relevant limit states is investigated.

The built-up I-shape investigated has F_y = 50 ksi, web thickness of t_w = 0.25 in., flange thickness of t_f = 0.50 in., and does not have transverse stiffeners. The overall depth of the member, d, was

varied. In the CBFEM model, the I-shape was modeled as two segments CJP welded to each other subject to uniform shear with a buckled shape as shown in Figure 8.

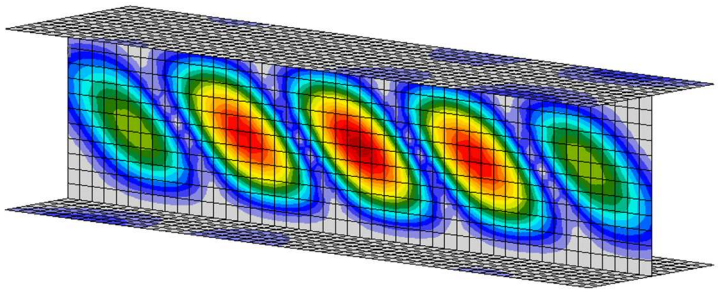

Figure 8: Buckled shape for shear buckling in a built-up I-shaped member

Results for this connection are shown in Figure 9 with respect to the width-to-thickness ratio of the web, h/t_w where $h = d–2t_f$. The results are normalized by the area of the web, $A_w = dt_w$, so that the yielding strength is constant. The design strength, ϕV_n, was computed using the provisions of AISC *Specification* (2022) Section G3. The elastic buckling strength, V_{el}, was computed as the critical buckling stress from Eq. 4 with k = 8.98, a value appropriate for an unstiffened plate clamped on two opposite edges and simply supported on the remaining two edges (Young et al. 2011), and $b/t = h/t_w$ times the area of the web.

The normalized design yielding strength is constant at $\phi 0.6F_y$ and the normalized CBFEM yielding strength is constant at a slightly lower value. The CBFEM buckling stress is somewhat lower than the approximate value used in this study. With $\alpha_{cr,lim} = 3.0/\phi$, as shown in Figure 9(a), the CBFEM design strength is accurate or conservative in comparison to the AISC design strength across the whole range of width-to-thickness ratios. A value of $\alpha_{cr,lim} = 2.1/\phi$, as shown in Figure 9(b), provides improved CBFEM results with the transition between yielding and buckling controlling the traditional calculations occurring at approximately the same width-to-thickness ratio as the transition between the plastic strain limit and the critical buckling ratio limit controlling for CBFEM.

5. Web Local Crippling

Web local crippling can occur in slender webs with compressive concentrated forces. Provisions for web local crippling are in AISC *Specification* (2022) Section J10.3. According to the commentary on the AISC *Specification* "web local crippling was defined as a crumpling of the web into buckled waves directly beneath the load". However, testing has also shown a single bulge in the web beneath the load.

Web local crippling is investigated here for a built-up I-shaped member supporting a column where web local crippling and web local yielding are the relevant limit states. The built-up I-shape investigated has F_y = 50 ksi, overall depth of d = 18 in., flange thickness of t_f = 1.0 in., bearing length of l_b = 12 in., and does not have transverse stiffeners. The web thickness, t_w, was varied. In the CBFEM model, the I-shape supports a W10×45 wide flange column with a 1 in. thick base plate. The buckled shape of the connection is shown in Figure 10.

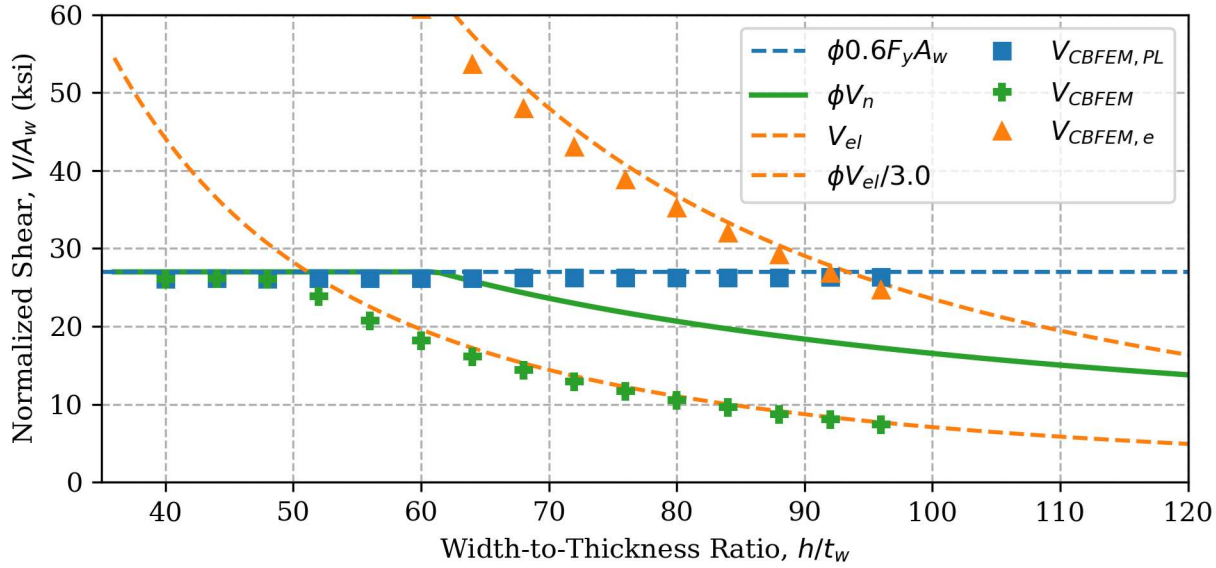

(a) with $\alpha_{cr,lim} = 3.0/\phi$

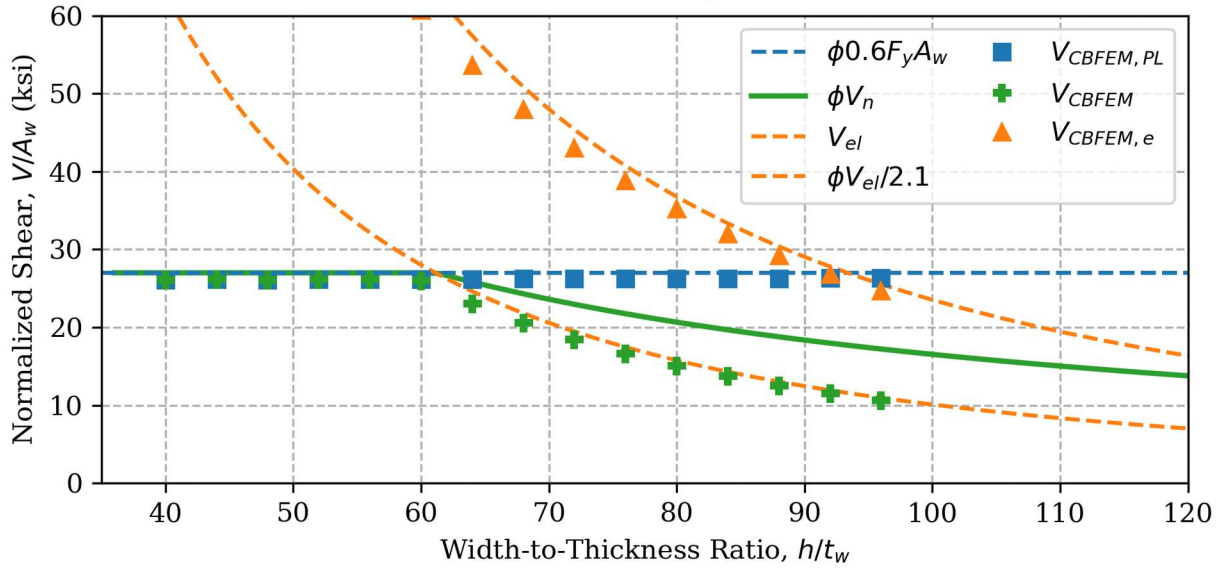

(b) with $\alpha_{cr,lim} = 2.1/\phi$

Figure 9: Strength comparison for shear buckling in a built-up I-shaped member

Results for this connection are shown in Figure 11 with respect to the width-to-thickness ratio of the web, h/t_w where $h = d–2t_f$. The results are normalized by the design strength for the limit state of web local yielding, $\phi R_{n,WLY}$, calculated according to the provisions of AISC *Specification* (2022) Section J10.2, so that the yielding strength is constant. The design strength, ϕR_n, was computed as the minimum of the design strengths for web local yielding and web local crippling [i.e., $\phi R_n = \min(\phi R_{n,WLY}, \phi R_{n,WLC})$ where $\phi R_{n,WLC}$ is calculated according to the provisions of AISC *Specification* Section J10.3]. The elastic buckling strength, P_{el}, was curve fit to the values of $P_{CBFEM,e}$ and thus does not represent an independent result as is the case for the other connections evaluated in this study. Note that the resistance factor for web local yielding is $\phi = 1.00$, the resistance factor for web local crippling is $\phi = 0.75$, the resistance factor used in the critical buckling ratio limit was $\phi = 0.90$, and the material strength reduction used in the CBFEM analysis was $\phi = 0.90$.

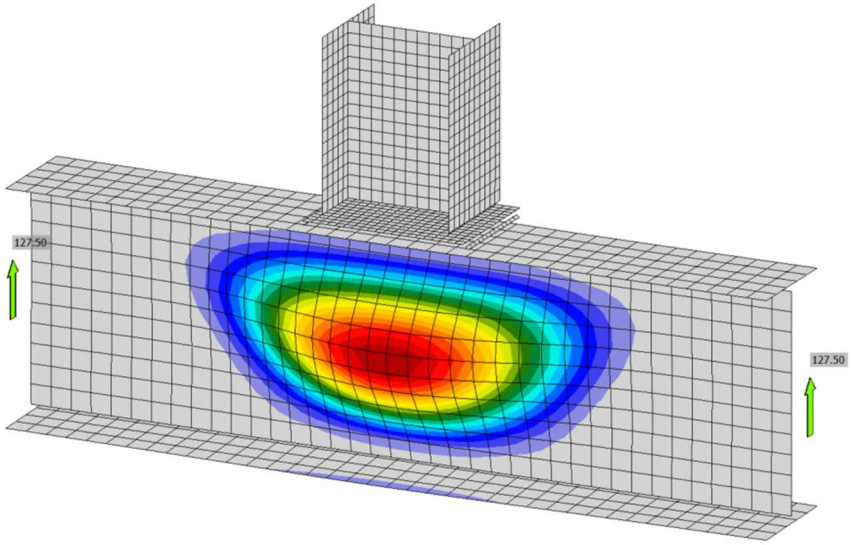

Figure 10: Web crippling in a built-up I-shaped member

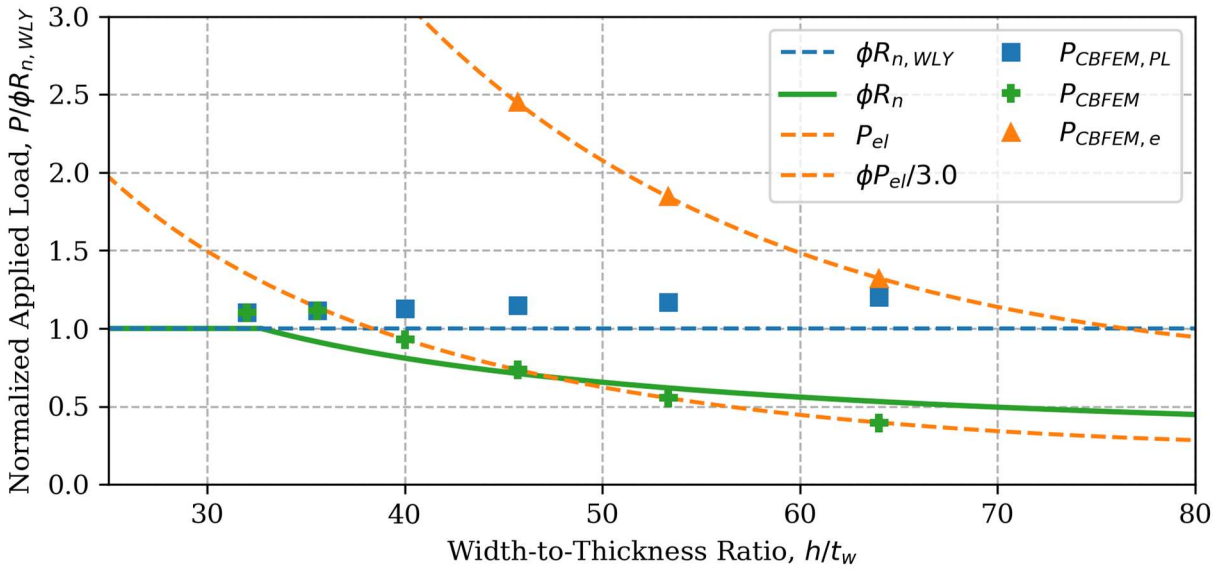

Figure 11: Strength comparison for web crippling in a built-up I-shaped member

As normalized in Figure 11, the design yielding strength is constant at unity. The CBFEM yielding strength is somewhat higher than unity representing differences between the traditional method and the CBFEM in the evaluation of the web local yielding limit state. With $\alpha_{cr,lim} = 3.0/\phi$, the CBFEM design strength provides a reasonable approximation for the AISC design strength across the whole range of width-to-thickness ratios. A higher value of the limit would provide more conservative results.

6. Conclusions

Nonlinear analysis is a powerful tool for structural design, including for design of structural steel connections. However, analysis capabilities available for design office use are not yet to a point where all the effects that impact the stability of structural steel connections can be modeled efficiently. As a result, there is a need for simplified methods of assessing buckling that ensure

safety. One such approach is the use of a critical buckling ratio limit where the ratio between critical buckling load from a linear bifurcation analysis and the applied load is not allowed to exceed a specific value. This approach was evaluated through comparisons between results from the component-based finite element method (CBFEM) and traditional code provisions for several stability limit states. The approach is effective; however, the appropriate limiting critical buckling ratio was seen to vary with failure mode, connection configuration, and material properties. Without a priori knowledge of an appropriate limiting critical buckling load, engineers should use conservative upper bounds. For the investigated cases with F_y = 50 ksi, limits of 3.0/ϕ for LRFD or 3.0Ω for ASD when the element is supported on three or four edges and 9.0/ϕ for LRFD or 9.0Ω for ASD when the element is supported on two edges (where ϕ = 0.90 and Ω = 1.67) are appropriate. These recommendations can be improved with further investigation including through comparisons to experimental results.

Acknowledgments
Funding for this study was provided by IDEA StatiCa and project No. LUAUS23114 in program INTER-ECELLENCE II – subprogram INTER-ACTION – LUAUS23 of the Czech Ministry of Education, Youth and Sports. The opinions expressed in this paper are those of the authors and do not necessarily reflect the views of the sponsors.

References
AISC. (2022). *Specification for Structural Steel Buildings*. ANSI/AISC 360-22, American Institute of Steel Construction, Chicago, Illinois.

CEN. (2005). *Eurocode 3: Design of steel structures – Part 1-1: General rules and rules for buildings*. EN1993-1-1, European Committee for Standardization, Brussels, Belgium.

Denavit, M. D., Nassiri, A., Mahamid, M., Vild, M., Wald, F., and Sezen, H. (2024). *Steel Connection Design by Inelastic Analysis*. John Wiley & Sons, Inc., Hoboken, New Jersey.

Dowswell, B. (2016). "Stability of Rectangular Connection Elements." *Engineering Journal*, AISC, 53(4), 171–202.

Dowswell, B., and Vild, M. (2023). "Linear buckling analysis in the design of bracket plates." *ce/papers*, 6(3–4), 1831–1836.

IDEA StatiCa. (2023). "Global buckling vs. local buckling. What does it mean?" *IDEA StatiCa*, <https://www.ideastatica.com/support-center/global-buckling-vs-local-buckling-what-does-it-mean>.

Wald, F., Šabatka, L., Bajer, M., Jehlička, P., Kabeláč, J., Kožich, M., Kuříková, M., and Vild, M. (2020). *Component–Based Finite Element Design of Steel Connections*. Czech Technical University in Prague.

Young, W., Budynas, R., and Sadegh, A. (2011). *Roark's Formulas for Stress and Strain, 8th Edition*. McGraw Hill, New York.